

A multi-stage design framework for the investment and operation of a simple microgrid: a comprehensive approach

Hugo Radet, Xavier Roboam, Bruno Sareni, Rémy Rigo-Mariani

▶ **To cite this version:**

Hugo Radet, Xavier Roboam, Bruno Sareni, Rémy Rigo-Mariani. A multi-stage design framework for the investment and operation of a simple microgrid: a comprehensive approach. Symposium du Génie Electrique, Jul 2021, Nantes, France. hal-03294283

HAL Id: hal-03294283
https://hal.science/hal-03294283

Submitted on 21 Jul 2021

HAL is a multi-disciplinary open access archive for the deposit and dissemination of scientific research documents, whether they are published or not. The documents may come from teaching and research institutions in France or abroad, or from public or private research centers.

L'archive ouverte pluridisciplinaire **HAL**, est destinée au dépôt et à la diffusion de documents scientifiques de niveau recherche, publiés ou non, émanant des établissements d'enseignement et de recherche français ou étrangers, des laboratoires publics ou privés.

A multi-stage design framework for the investment and operation of a simple microgrid: a comprehensive approach.

Hugo RADET[†], Xavier ROBOAM[†], Bruno SARENI[†], Rémy RIGO-MARIANI[*]
[†] LAPLACE, Univ. Toulouse, CNRS, INPT, Toulouse, France
[*] G2Elab, Univ. Grenoble Alpes, CNRS, INPG, Grenoble, France

Abstract – Investment and operation of microgrids are challenging, especially when dealing with large-scale problems. As a result, optimization approaches are commonly used to tackle this issue. While most studies do not take renewal investment into account, this paper addresses the dynamic (multi-stage) investment and operation of a simple microgrid including Li-ion batteries and solar panels. Because the investment dynamic is a slow process compared to the operation, two time scales are introduced to formulate the problem. We show how to bridge the gap between these two time scales in order to ensure time continuity. Then, the problem is solved in a deterministic framework by using Mixed-Integer-Linear-Programming (MILP) for both time scales. Clustering methods are also introduced to reduce the computational complexity of the problem by reducing the length of the simulation periods (in terms of time steps). The multi-stage approach not only optimizes the size of technologies, but also determines the investment pathway along the horizon depending on the techno-economic objective.

Keywords – microgrids, techno-economic, multi-stage investment, mixed-integer-linear-programming (MILP)

1. INTRODUCTION

The sizing and operation of energy systems are challenging because of the problem complexity which rapidly grows with the number of time steps and uncertainties that arise from multiple time scales. To tackle this issue, various methodologies have already been proposed and Connolly et al. [1] made a fair review of the existing modeling tools to deal with the analysis of energy systems. The problem is usually simplified (by mean of linearization techniques or reduced simulation period, for example) depending on the aim of the study in order to make it computationally tractable. As a result, the investment is most of time treated as a static variable while system aging is neglected. The design is only made once at the beginning of the study. However, when the study horizon is longer than 15 years, replacements usually occur and new investment decisions have to be made. For instance, in [2, 3] the authors do not account for dynamic investment in the optimization. Instead, the equivalent annual investment cost is minimized in order to have reasonable computational times. They both use mixed-integer linear programming (MILP) formulation for the optimization with piecewise linearization to account for non-linearities. While most of the studies [4] implement mathematical programming techniques where the model equations are considered as constraint of optimization problems, other approaches [5, 6] use (meta)heuristics for both the investment and operation. This choice is usually made because of high detailed models where linearization or convex relaxations are not always an easy task. Investment is again a static decision variable computed by black-box functions integrated in evolutionary methods such as genetic algorithms. When replacements are taken into account in the economic analysis, they are usually deduced from extrapolation on a single simulation year and their costs are computed a posteriori. To our knowledge, only [7] tackles the problem using a two time scale formulation in a stochastic framework for the long term management of energy storage. The formulation of this paper is based on their work and applied to the design and operation of a simple microgrid in a deterministic framework.

The main objective of this work is to write down a comprehensive formulation of the problem by introducing two time

Sets		
$h \in \mathbb{H}$	Set of hours	
$d \in \mathbb{D}$	Set of days	
$y \in \mathbb{Y}$	Set of years	
$td \in \mathbb{TD}$	Set of typical days	
$tb \in \mathbb{TB}$	Set of time blocks	
Operation variables		
$p^{pv}_{h,y}$	PV power	[kW]
$p^{pv,curt}_{h,y}$	PV curtailed power	[kW]
$p^{b,+}_{h,y}$, $p^{b,-}_{h,y}$	Battery charge/discharge power	[kW]
$p^{g,+}_{h,y}$	Grid power	[kW]
$soc^{b}_{h,y}$	Battery state of charge	[kWh]
$soh^{b}_{h,y}$	Battery state of health	[kWh]
Investment variables		
r^{pv}_{y}	New PV size	[kWc]
r^{b}_{y}	New battery size	[kWh]
p^{peak}_{y}	PV peak power	[kWc]
E^{b}_{y}	Battery capacity	[kWh]
Parameters		
τ	Discount rate	[0,1]
η^{-}, η^{+}	Battery charge/discharge efficiencies	[0,1]
$\underline{\alpha^{soc}}$, $\overline{\alpha^{soc}}$	Battery lower/upper SoC bound factors	[0,1]
$\underline{\alpha^{p}}$, $\overline{\alpha^{p}}$	Battery lower/upper power bound factors	[h^{-1}]
n_c	Battery max. number of cycles	[-]
dod	Battery depth-of-discharge	[0,1]
$p^{ld}_{h,y}$	Load input profile	[kW]
$p^{pv,norm}_{h,y}$	PV normalized input profile	[pu]
τ^{self}_{y}	Self-sufficiency ratio	[0,1]
$\overline{r^{pv}_{y}}$	New PV size bound	[kWc]
$\overline{r^{b}_{y}}$	New battery size bound	[kWh]
$n_{td,y}$	Number of days in cluster td for year y	[-]
n_{tb}	Number of years in time block tb	[-]
C^{pv}_{y}	PV investment cost for year y	[€/kWc]
C^{b}_{y}	Battery investment cost for year y	[€/kWh]
$C^{g,+}_{y}$	Tariff of electricity for year y	[€/kWh]

Table 1. Nomenclature for the multi-stage problem

scales for both the investment and the operation, treated as dynamic variables. The scope of this paper is limited to the deterministic case where all the data (i.e. load/renewable profiles, energy prices and equipment costs) are supposed to be completely known over the horizon (perfect foresight). A single MILP formulation is proposed to solve the problem. Clustering methods are also introduced in order to limit computational times by reducing the length of the simulation period. The main contribution of the paper being the used methodology, the case study remains simple with Li-ion batteries and solar panels designed for a small office. To summarize, the main contributions of this work are:

- Inclusion of dynamic investment into MILP formulation and its implications in terms of design and operation.
- The coupling of this approach with clustering methods to reduce computational times.

The paper is organized as follows: section 2 shows the problem formulation for multi-stage investment. Next, clustering methods are introduced in section 3. Finally, results are shown in section 4 and conclusions and perspectives are drawn in section 5.

2. MATHEMATICAL FORMULATION

2.1. *Notations*

The investment dynamic is a slow process compared to the operation where power flow decisions need to be made every hours. Hence, we define two time scales denoted by $y \in \{1, \dots, Y\}$ and $h \in \{1, \dots, H\}$ with Δ_y and Δ_h the two time steps respectively. We assume that y is the investment/slow time scale (in years) and h the operation/fast time scale (in hours). A time continuum is ensured as depicted in figure 1. The problem is formulated in a state/decision framework [8]. States are denoted by $x \in \mathbb{X}$ while decisions by $u \in \mathbb{U}$.

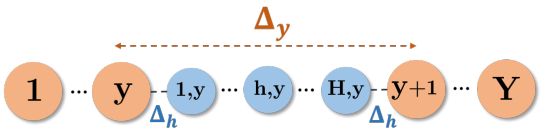


Figure 1. A time continuum is ensured in the simulation between the investment (y) and operation (h) time scale

Power flows are counted positive for generation except for the load which is in passive sign convention.

2.2. *Operation time-scale*

At the operation time-scale, decision variables of the problem are the power flows controlled in the microgrid which are the charge/discharge powers of the battery $p^{b,-}_{h,y}, p^{b,+}_{h,y}$ and the curtailed solar power $p^{pv,curt}_{h,y}$. They are arranged in the decision vector (1) and their limits are represented by constraints (2), (3) and (4). The grid power $p^{g,+}_{h,y}$ is introduced to make the optimization implementation clearer but it is not a degree of freedom of the problem. This latter quantity is also limited (5) by the maximum power allowed by the external network.

$$u^o_{h,y} = \begin{pmatrix} p^{b,-}_{h,y} & p^{b,+}_{h,y} & p^{pv,curt}_{h,y} \end{pmatrix} \tag{1}$$

The energy demand is given by $p^{ld}_{h,y}$ and the solar production $p^{pv}_{h,y}$ is given by equation (6) where the input normalized generation profile $p^{pv,norm}_{h,y}$ is multiplied by the peak power $p^{pv,peak}_y$.

$$-p^{pv}_{h,y} \leq p^{pv,curt}_{h,y} \leq 0 \tag{2}$$

$$0 \leq p^{b,+}_{h,y} \leq \overline{\alpha^p} \cdot E^b_y \tag{3}$$

$$\underline{\alpha^p} \cdot E^b_y \leq p^{b,-}_{h,y} \leq 0 \tag{4}$$

$$0 \leq p^{g,+}_{h,y} \leq \overline{p^g} \tag{5}$$

$$p^{pv}_{h,y} = p^{pv,peak}_y \cdot p^{pv,norm}_{h,y} \tag{6}$$

A minimum self-sufficiency ratio $\tau^{self}_y \in [0,1]$ is introduced as a parameter in the constraint (7). This latter quantity is defined as a ratio of the energy use from on-site generation to the total energy demand [9]. A ratio equal to 1 means that all the electricity consumed is provided by the installed solar panels.

$$\sum_{h=1}^{H} (p^{g,+}_{h,y} \cdot \Delta_h) \leq (1 - \tau^{self}_y) \cdot \sum_{h=1}^{H} (p^{ld}_{h,y} \cdot \Delta_h) \tag{7}$$

State variables are the battery state of charge (SoC) and state of health (SoH). The SoC dynamic is given by equation (8) where η^- and η^+ are the charging and discharging efficiencies respectively. To avoid fast aging due to deep charge and discharge, the SoC has to remain between upper and lower bounds (usually set to 80% and 20% of the battery capacity, respectively) as it is commonly done for Li-ion batteries (9).

$$soc^b_{h+1,y} = soc^b_{h,y} - (\eta^- \cdot p^{b,-}_{h,y} + \frac{p^{b,+}_{h,y}}{\eta^+}) \cdot \Delta_h \tag{8}$$

$$\underline{\alpha^{soc}} \cdot E^b_y \leq soc^b_{h,y} \leq \overline{\alpha^{soc}} \cdot E^b_y \tag{9}$$

The battery SoH is computed using a simple model based on the maximum exchangeable energy during its lifespan [10]. This model only considers aging due to cycling. Calendar aging mostly depends on the ambient temperature conditions, thus we assume that the temperature is controlled in order to neglect this latter contribution. Furthermore, battery parameters such as loss of capacity or increase of internal resistance over time are not taken into account as a first approximation. The maximum exchangeable energy is then given by $\overline{soh^b_y} = 2 \cdot n_c \cdot dod \cdot E^b_y$ which depends on the battery maximum number of cycles n_c for a fixed depth-of-discharge dod. The dynamic is given by equation (10). The battery is renewed whenever the SoH reaches zero. Thus, its value has to remain positive (11).

$$soh^b_{h+1,y} = soh^b_{h,y} - (p^{b,+}_{h,y} - p^{b,-}_{h,y}) \cdot \Delta_h \tag{10}$$

$$0 \leq soh^b_{h,y} \leq \overline{soh^b_y} \tag{11}$$

Finally, the power balance is ensured by (12).

$$p^g_{h,y} + p^{pv}_{h,y} + p^{pv,curt}_{h,y} + p^{b,+}_{h,y} + p^{b,-}_{h,y} = p^{ld}_{h,y} \tag{12}$$

2.3. *Investment time-scale*

At the investment time scale, the decision variables are the new capacity installed for the battery r^b_y and the new peak power r^{pv}_y for solar panels that could be made every year (13).

$$u^i_y = \begin{pmatrix} r^b_y & r^{pv}_y \end{pmatrix} \tag{13}$$

They are both continuous, positive and bounded variables to reduce the search space (14), (15).

$$0 \leq r^{pv}_y \leq \overline{r^{pv}} \tag{14}$$

$$0 \leq r^b_y \leq \overline{r^b} \tag{15}$$

In order to properly model the replacement dynamic, a difference is made between the new design of systems and the existing system sizes which have to be updated when investment decisions are made. Thus, unlike static investment optimization, state variables are also introduced for the investment. Technology sizes could be increased or downscaled depending on the case study. Hence, when an investment decision is made, system sizes E_y^b and $p_y^{pv,peak}$ need to be updated with the new installed capacities. Otherwise, they remain the same as the year before. This investment dynamic is given by (16) and (17).

$$p_{y+1}^{pv,peak} = \begin{cases} r_y^{pv}, \text{ if } r_y^{pv} > 0 \\ p_y^{pv,peak}, \text{ otherwise} \end{cases} \tag{16}$$

$$E_{y+1}^{b} = \begin{cases} r_y^{b}, \text{ if } r_y^{b} > 0 \\ E_y^{b}, \text{ otherwise} \end{cases} \tag{17}$$

Big-M values with binary variables are introduced in order to linearize if-else functions as it is commonly done in MILP formulation. As an example, the investment dynamic equation (17) for the battery becomes:

$$\begin{aligned} E_{y+1}^b - r_y^b &\leq M \cdot (1 - \delta_y^b) \\ r_y^b - E_{y+1}^b &\leq M \cdot (1 - \delta_y^b) \\ E_{y+1}^b - E_y^b &\leq M \cdot \delta_y^b \\ E_y^b - E_{y+1}^b &\leq M \cdot \delta_y^b \end{aligned} \tag{18}$$

where M is the big-M value and δ_y^b a binary variable which is equal to 1 when $r_y^b > 0$. The same procedure applies for equation (16). Note that the computational times are greatly sensitive to the value of M as the optimization search space depends on its value.

2.4. *Bridging the gap between time-scales*

Both operation and investment decisions have to be made over the horizon but at different time scales. To ensure time continuity between years for the battery SoC and the SoH, the decision process is defined as follows: investment decisions are made at **the end of the last hour of each year** (H, y) when the SoH and SoC are completely known over the year. The design of the assets are then updated with the new sizes at the beginning of the first hour of the next year $(1, y+1)$. Furthermore, the new battery which is installed is assumed to be fully charged with a maximum exchangeable energy. Thus, continuity equations for the SoH and SoC between years are given by (19) and (20).

$$soc_{1,y+1}^b = \begin{cases} \overline{soc^b} \cdot r_y^b, \text{ if } r_y^b > 0 \\ soc_{H+1,y}^b, \text{ otherwise} \end{cases} \tag{19}$$

$$soh_{1,y+1}^b = \begin{cases} 2 \cdot n_c \cdot dod \cdot r_y^b, \text{ if } r_y^b > 0 \\ soh_{H+1,y}^b, \text{ otherwise} \end{cases} \tag{20}$$

The same big-M method is applied to linearize (19) and (20).

2.5. *Objective function*

In the following, the objective of the optimization problem is to minimize the discounted sum of both the investment cost and operation cost over the horizon (21).

$$\underbrace{\sum_{y=1}^{Y} \gamma_y \left(\underbrace{c_y^{pv} \cdot r_y^{pv} + c_y^b \cdot r_y^b}_{\text{Investment cost}} + \sum_{h=1}^{H} \underbrace{c_{h,y}^{g,+} \cdot p_{h,y}^{g,+} \cdot \Delta_h}_{\text{Operation cost}} \right)}_{\text{Annual discounted cost}} \tag{21}$$

where c_y^{pv} and c_y^b are the investment cost of solar panels (€/kWc) and the battery (€/kWh) respectively. The tariff of electricity (€/kWh) purchased from the external network is given by $c^{g,+}$ as we assume that no electricity could be sold to the grid. Note that these latter quantities could change over the horizon as they are also indexed by y. The value of the discount factor γ_y is given by (22).

$$\gamma_y = \frac{1}{(1+\tau)^y} \tag{22}$$

where τ is the discount rate.

3. TIME BLOCKS AND TYPICAL DAYS TO LIMIT COMPUTATIONAL TIME

When the multi-stage approach is applied directly to the whole 20 years horizon at a hourly time step, the problem is too big to be directly solved in less than one day with a standard computer. Hence, to reduce computational times, representative periods are introduced at both investment and operation time scales:

- Similar consecutive years could be clustered into time blocks represented by a single representative year of data.
- Similar days are clustered into typical day (TD) classes.

In this section clustering methods are first introduced to select representative periods. Then, we show how to choose the right sets for optimization variables in order to include these periodicity classes into optimization.

3.1. *Clustering method*

Several clustering methods have been developed to reduce the time horizon by extracting representative periods from the original dataset [11, 12]. For instance, [2, 13] implemented these methods to select typical days from a set of weather and energy demand time series. The standard clustering framework has been developed by Teichgraeber et Brandt [12] and could be summed up as follows (see figure 2):

1. *Normalization:* time series are normalized when using multiple data sets with different units and combined to keep the synchronicity between the production and demand.
2. *Assignement:* clusters are identified by grouping similar periods each others.
3. *Representation:* each period of the time series is associated to a cluster and the sequence of clusters is deduced. Then, representative periods are obtained by denormalization.

Among those clustering methods, the k-means algorithm is chosen. Further details about the k-means algorithm and clustering methods could be found in the following reference [12].

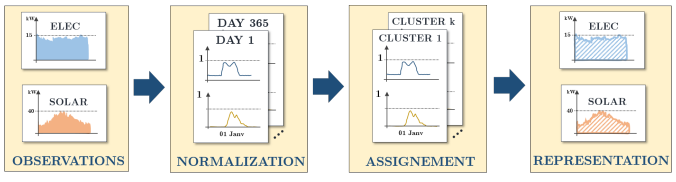


Figure 2. Clustering process to select representative days.

3.2. *Time blocks at the investment time scale*

When dealing with long term horizon, the number of investment stages could lead to intractable computational time as state variables should be computed for each and between consecutive years to ensure time continuity. One way to tackle this issue is to consider that the energy demand, the solar production and

the cost of technologies are the same over periods of multiple years. Hence, the horizon could be divided into time blocks $tb \in \{1, ..., TB\}$ which are groups of years represented by a single year of data (figure 3). Therefore, while operation decisions are made over the representative year, investment decisions are only made at the end of every time block instead of every year. Furthermore, this assumption is not inconsistent with the fact that since a system has been installed, its lifespan is usually longer than a single year, thus considering yearly updates of the equipment may not be relevant.

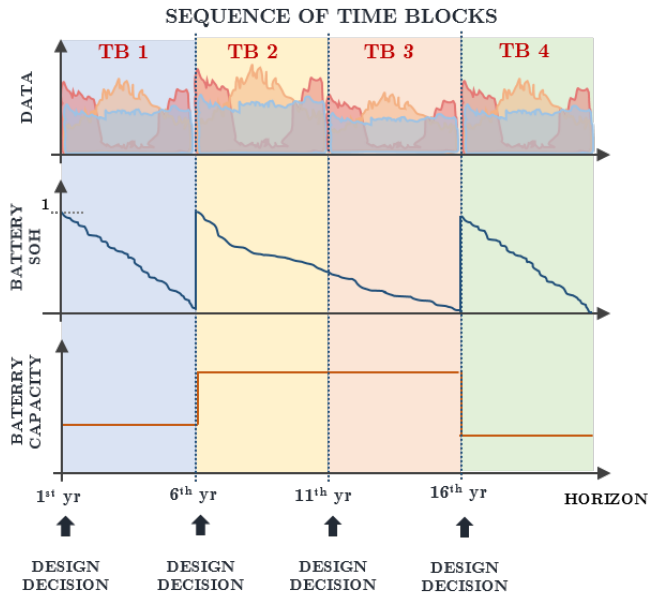


Figure 3. Schematic view of the time blocks representation of the horizon. Design decisions are made at the end of the time block interval. Time continuity is ensured for the SoH and the capacity between time blocks. The SoH is equal to 1 when a new battery is installed.

How does it work on a 20-years horizon study where investment decisions are assumed to be made every 5 years? The horizon is split as shown in figure 3. The first investment decision is made at the end of the first year as previously mentioned. From the figure above, the horizon is divided into 4 time blocks and the sequence of decisions given by:

$$1 \rightarrow 2 \rightarrow 3 \rightarrow 4$$

matches to the following sequence when time blocks are divided into years:

$$1 \rightarrow 6 \rightarrow 11 \rightarrow 16$$

Since the operation state variables are only computed on a single representative year while representing multiple years, some continuity issues have to be tackled:

- Continuity equations to bridge the gap between time scales are unchanged except that consecutive years are replaced by consecutive time blocks.
- Every years of a given time block are assumed to be similar. Thus, a periodic constraint is added to the SoC (23).

$$soc^b_{H+1,tb} = soc^b_{1,tb} \tag{23}$$

- Because of the linear SoH dynamic, this latter is multiplied at each time step by the time block number of years. Equation (10) becomes (24):

$$soh^b_{h+1,tb} = soh^b_{h,tb} - n_{tb} \cdot (p^{b,+}_{h,tb} - p^{b,-}_{h,tb}) \cdot \Delta_h \tag{24}$$

where n_{tb} is the time block number of years.

- In the objective function, the operation cost is multiplied by the number of years in the given time block (25).

$$\sum_{tb=1}^{TB} \gamma_{tb} \left(c^{pv}_{tb} \cdot r^{pv}_{tb} + c^{b}_{tb} \cdot r^{b}_{tb} + n_{tb} \sum_{h=1}^{H} c^{g,+}_{h,tb} \cdot p^{g,+}_{h,tb} \cdot \Delta_h \right) \tag{25}$$

3.3. *Typical days at the operation time scale*

Most of the time, instead of computing operation variables along the 8760 hours, a set of typical days/weeks is identified and both decisions and state variables are computed independently over this set. However, no dynamics between days could be modeled by this approach. Gabrielli et al [2] show that despite great computational time improvement, this latter approach underestimates sizing values compared to the reference case where the problem is formulated over the whole time horizon. This latter conclusion holds particularly when the energy system includes seasonal storage. Hence, they proposed a novel method by coupling typical days to take inter days dynamics into account. To this end, only state variables are computed over the 8760h while decision variables are only computed on the typical day set. The coupling is essentially based on the sequence of typical days obtained from clustering. Computation time improvement is lower than the former method but the design seems to be better approximated. The coupling method is illustrated in figure 4 and could be summarized as follows:

- Power decisions are only computed for each hours of each typical days $td \in \{1, .., TD\}$ of year y.
- State variable dynamics are computed each hour of each day $d \in \{1, .., D\}$ over the horizon from the sequence of typical days σ_y of year y.
- For state variables, one more constraint is added to ensure time continuity between days: the value at the end of day d is equal to the value at the beginning of day $d + 1$.

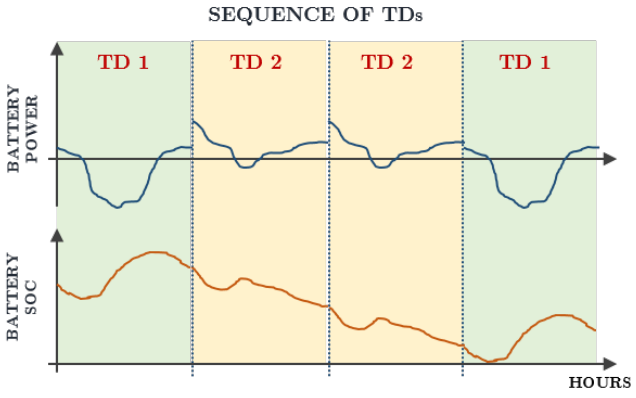


Figure 4. Schematic view of the typical day representation over 4 days. Each day is associated to one cluster (typical day). The upper figure represents the power decision which is the same for each given typical days. Its value is negative when charging and positive otherwise. The lower figure is the SoC constraint evolution where continuity is ensure between days from the sequence of TD.

This method is applied to the multi-stage formulation. Therefore, the set of hours now represents the 24 hours of the day. Decision variables are also indexed by the typical day index so that the power balance becomes:

$$p^{g}_{h,td,y} + p^{pv}_{h,td,y} + p^{pv,curt}_{h,td,y} + p^{b,+}_{h,td,y} + p^{b,-}_{h,td,y} = p^{ld}_{h,td,y} \tag{26}$$

State equations (8) and (10) becomes:

$$soc^b_{h+1,d,y} = soc^b_{h,d,y} - (\eta^- \cdot p^{b,-}_{h,\sigma_y(d),y} + \frac{p^{b,+}_{h,\sigma_y(d),y}}{\eta^+}) \cdot \Delta_h \quad (27)$$

$$soh^b_{h+1,d,y} = soh^b_{h,d,y} - (p^{b,+}_{h,\sigma_y(d),y} - p^{b,-}_{h,\sigma_y(d),y}) \cdot \Delta_h \quad (28)$$

Where $\sigma_y(d)$ gives the typical day associated to day d for year y, thus $p^b_{h,\sigma_y(d),y}$ is the battery power associated to the $\sigma_y(d)$ typical day. The following constraints are added to ensure the coupling between days:

$$soc^b_{1,d+1,y} = soc^b_{H+1,d,y} - (\eta^- \cdot p^{b,-}_{1,\sigma_y(d+1),y} + \frac{p^{b,+}_{1,\sigma_y(d+1),y}}{\eta^+}) \cdot \Delta_h \quad (29)$$

$$soh^b_{1,d+1,y} = soh^b_{H+1,d,y} - (p^{b,+}_{1,\sigma_y(d+1),y} - p^{b,-}_{1,\sigma_y(d+1),y}) \cdot \Delta_h \quad (30)$$

Finally, concerning the objective function, the operation cost for each typical day is multiplied by $n_{td,y}$ which is the number of days related to the cluster td of year y (31).

$$\sum_{y=1}^{Y} \gamma_y \Big(c^{pv}_y \cdot r^{pv}_y + c^b_y \cdot r^b_y + \sum_{td=1}^{TD} n_{td,y} \big(\sum_{h=1}^{H} c^{g,+}_{h,td,y} \cdot p^{g,+}_{h,td,y} \cdot \Delta_h \big) \Big) \quad (31)$$

3.4. *Coupling the previous simplifications approaches*

When coupling the time block and typical day approximations, index y becomes tb and the n_{tb} factor is added to the previous objective function (32).

$$\sum_{tb=1}^{TB} \gamma_{tb} \Big(c^{pv}_{tb} \cdot r^{pv}_{tb} + c^b_{tb} \cdot r^b_{tb} + n_{tb} \sum_{td=1}^{TD} n_{td,tb} \big(\sum_{h=1}^{H} c^{g,+}_{h,td,tb} \cdot p^{g,+}_{h,td,tb} \Delta_h \big) \Big) \quad (32)$$

4. NUMERICAL RESULTS

4.1. *Case study*

Input data and variables are listed below:

- The electrical demand comes from an office building located in Seattle and provided by the U.S department of energy (DOE). It is part of the reference building benchmark datasets, simulated thanks to the EnergyPlus software and freely available from the openEI portal [14]. Solar radiation comes from the TMY file uploaded to simulate the building energy consumption. The PVlib [15] software is then used to convert solar data into power production and the resulting values were normalized.
- The tariff of electricity follows a peak/off-peak EDF 36 kVA "Tarif Bleu" [16].
- The cost of storage system (Li-ion battery + converter) is given by [17] and decreases from 600 €/kWh in 2021 to 300 €/kWh in 2040.
- The cost of solar panels including AC/DC converters is given by [18] and decreases from 1040 €/kWc in 2021 to 735 €/kWc in 2040.
- The discount rate τ is set to 4.5%.
- Technical parameters for the battery are reported in table 2.
- The energy demand is first assumed to be the same over the 20 years.

The problem is modeled using Julia and JuMP package. The CPLEX solver is then used to solve the problem. All the computations run on a Core i5 - 7200U CPU @ 2.5 GHz x 2 computer.

Param.	η^-	η^+	$\underline{\alpha^{soc}}$	$\overline{\alpha^{soc}}$	$\underline{\alpha^p}$	$\overline{\alpha^p}$	n_c
Battery	0.8	0.8	0.2	0.8	-1.5	1.5	5000

Table 2. Battery parameters

4.2. *Self-sufficiency ratio*

The Li-ion battery could cycle 5 000 times between 20% and 80% of its nominal capacity before replacement (assuming 1 cycle a day, its approximated lifetime is between 10 and 15 years), thus the horizon is divided into 2 time blocks and investment decisions are made the 1st and 11th year. Operation decisions are made each hours of the 365 days of a given time block.

Figure 5 shows the planning strategy over the horizon for the microgrid with a 60% self-sufficiency ratio. A 70 kWh battery and 60 kWc of PV are installed at the end of the first year. Then, the battery is renewed the 11th year when the SoH reaches zero (figure 6). Note that the optimizer does not take advantage of the investment cost decrease to increase the battery capacity when this latter has to be replaced. Instead, the capacity is slightly reduced so that the SoH of the renewed battery reaches zero at the end of the 20 years horizon. Otherwise, it would have led to a waste of "usable battery" with the considered problem formulation. Adding a salvage value (reward when the final battery SoH is positive at the end of the study) would probably change the results. Even with cost decrease and current energy prices, it is not economically profitable to purchase battery storage so that the optimizer installs just enough battery and PV to ensure the fulfillment of the self-sufficiency constraint. Figure 6 shows that the multi-stage formulation with time blocks decomposition handles correctly continuity issues and aging is controlled in order to install the new battery when the previous is out of order.

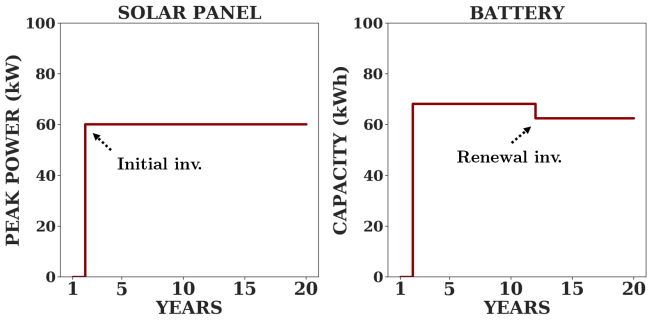


Figure 5. Planning strategy over the horizon with a 60% self-sufficiency ratio.

The impact of the self-sufficiency ratio on the design is assessed by varying this latter parameter from 40% to 100%. Results are depicted in figure 7. As we can observe, with 40% of self-sufficiency, only solar panels are installed while the battery remains too expensive. Then, until self-sufficiency reaches

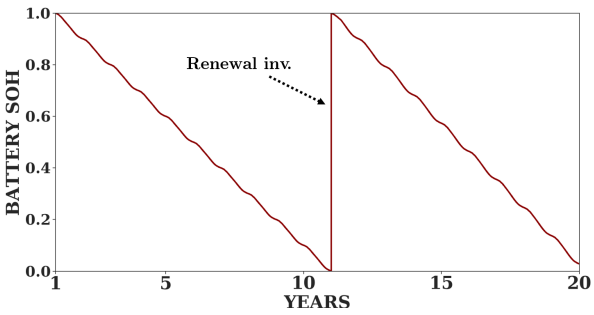


Figure 6. Battery SoH over the horizon with a 60% self-sufficiency ratio. The SoH has been normalized by the maximum exchangeable energy in the figure.

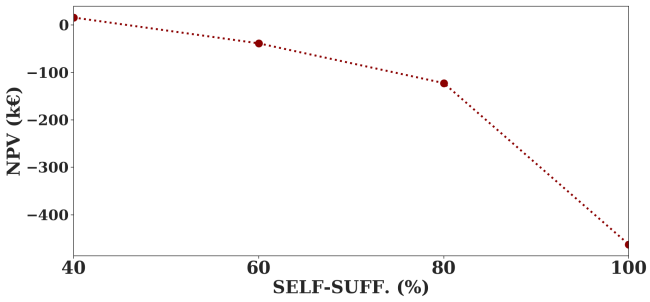


Figure 8. NPV evolution as a function of the self-sufficiency ratio.

80%, battery and solar panels are purchased and approximately the same capacity is installed when the battery is renewed. Finally, the sizing is exponentially increasing from 80% to 100%. This gap is mostly due to the need for oversized capacities in order to overcome extreme events where the production is low during long periods. As a result, the battery is mostly underused so that the maximum exchangeable energy is large enough to avoid any new costly replacement with the aging model developed in this work.

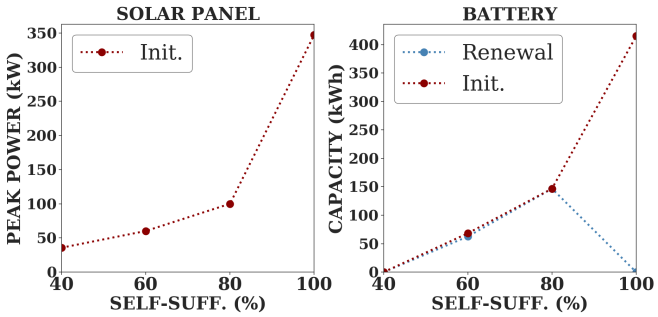
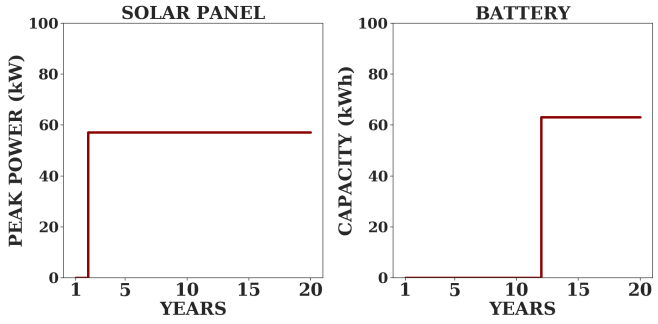


Figure 7. Design evolution as a function of the self-sufficiency ratio.

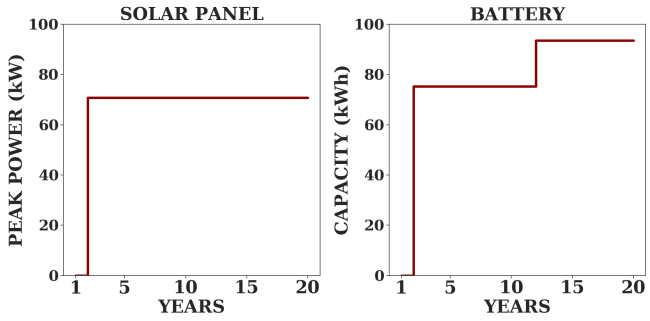
Finally, figure 8 shows the Net Present Value (NPV) evolution as a function of the self-sufficiency rate. This latter quantity is determined by computing the difference between positive cash flows and investment costs. A positive NPV results in profit: higher is the NPV at the end of the horizon, higher is profitability. In the study, cash flows correspond to savings compared to the case where all the electricity is bought from the grid. As shown in the figure, the microgrid is only profitable with a self-sufficiency ratio lower or equal to 40% with the cost assumptions made in this work. Then the NPV value goes rapidly negative, especially from 80% to 100% which is consistent with previous observations. Of course, self-sufficiency is not rewarded in that case study, the only positive cash flows are savings from the energy bill. To draw rigorous conclusions, a complete study has to be made but this point is out of the scope of this paper.

4.3. Electricity tariff

In this section, the self-sufficiency constraint is removed and the tariff of electricity is increased until a battery is installed at least once over the horizon. As shown in figure 9, a battery is purchased when the tariff of electricity is at least multiplied by 4. In that case, a battery is only installed at the beginning of the 12th year when the battery investment cost is approximately divided by 2. Unlike the static investment problem, the multi-stage approach gives at the same time the optimal design but also the optimal timing (investment pathway) to install the technology. When the tariff is multiplied by 5 (figure 9b), a first battery of 75 kWh is initially installed and replaced at the end of its lifespan (12th year) with a 95 kWh battery by taking full advantage of the cost decrease. Finally, the solar panel size increases when the electricity gets more costly, but no additional investment is made over the horizon. This latter aspect may be explained because when investment decisions are made, technologies are entirely replaced by new systems according to the modeling developed in this work. The cost induced is then proportional to new sizes instead of additional investment only. Thus, technologies with longer lifespan than the horizon are preferably installed the first year.



(a) Tariff multiplied by 4



(b) Tariff multiplied by 5

Figure 9. Design evolution as a function of the electricity tariff which is (a) multiplied by 4 and (b) multiplied by 5.

As shown in previous sections, the investment could whether be increased or downscaled by taking full advantage of the cost decrease and according to the energy supply constraints. The multi-stage approach increases the flexibility of the whole system as the investment can be adapted when strong evolutions occur. This flexibility improvement will be particularly interesting when uncertainties will be included in future works.

4.4. *Typical days*

The objective of this section is to study the impact of the typical day approximation on the design compared to the reference case where no clustering method is used. Gabrielli et al [2] show that in their case with static investment, the design of systems converge since the number of typical days is large enough to represent the entire set of data. The number of typical days needed to ensure convergence seems to be really case sensitive and no general conclusions could be drawn from their work. Hence, the same convergence study is applied to our benchmark where the self-sufficiency rate is fixed to 60%.

First, the k-means algorithm is run as previously mentioned in section 3 and the number of TD is set as a parameter. Figure 10 shows the duration curves for the input energy demand (left) and for the solar production (right), compared to the TD approximation curves. Without no surprise, when the number of TD grows, the curves are better approximated (see table 3) as the daily energy patterns diversity is increased.

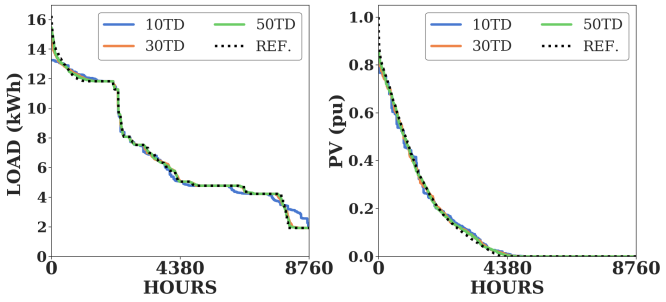


Figure 10. Load (left) and PV (right) duration curves comparison between the original dataset (ref) and the TD approximation with 10 (blue), 30 (orange) and 50 (green) typical days.

	10TDs	30TDs	50TDs
RMSE [kW]	0.35	0.21	0.15

Table 3. Load duration curve root mean square error between TD approximations and the reference case.

Figure 11 depicts the design comparison between the clustering and reference case. As shown in the figure, the objective cost is reaching a plateau with numbers of TD greater than 30. The relative error between the TD approximation and the reference cost objective is about 5% as shown in table 4. Concerning the size of systems, PV investment is slightly overestimated (relative error of 5%) when the number of TD is greater than 5 and its value remains approximately the same when the number of TD increases. In contrast, battery sizes for both initial and renewal investment do not converge to the reference value. Instead, both values reach a plateau which is lower than the reference sizes from about 10 kWh. To explain this gap, several hypothesis could be drawn: first, typical days for the PV do not display as much daily variations as the original data set which means that the direct self-consumption might be greater with the TD approximation. This latter point is even more reinforced as the energy demand profile comes from an office where most of the consumption happened during daylight. This hypothesis is also consistent with the overestimated PV size previously observed. Furthermore, peak demand and min/max variations are slightly underestimated with the TD approximation which may lead to lower purchased battery capacity. Future work may be conducted toward other clustering methods to verify those latter hypothesis.

With 30 typical days, computational times are approximately divided by 1.5 compared to the reference (see table 4). It seems that computational time are reduced since the number of TD

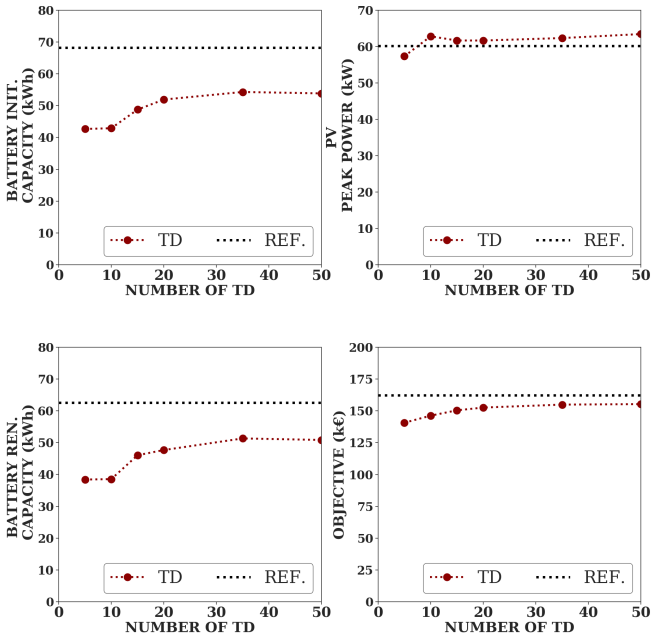


Figure 11. Design comparison between the TD approximation and the reference case as a function of the number of TDs.

	Ref.	10TDs	30TDs	50TDs
PV [kWc]	60	63	62	63
Batt. [kWh]				
Init.	68	43	54	54
Renewal	63	39	51	51
Obj. [k€]	162.4	146.2	154.9	155.3
CPU [min]	10.2	3.5	7.1	10.9

Table 4. Comparison of the results between the TD approximation and the reference case.

remains under 50. Otherwise, the complexity induced by the introduction of new sets and constraints probably compensate the computational gains brought by the TD approximation. Remind that computational times are not linear with the number of optimization variables but also depend on the way the problem is formulated. In this work, computational time were intentionally reduced even in the reference case to demonstrate the feasibility of the multi-stage approach. However, this TD simplification could make a great difference for long time computations since convergence has been proven. As previously mentioned, these conclusions are greatly case specific and results might be different with another benchmark. Finally, the typical days approach developed in this work would be even more relevant for energy systems including seasonal storage where the horizon should be at least equal to one year. This latter consideration will be treated in future works.

5. CONCLUSIONS

A generic multi-stage framework for both the design and operation of energy systems was presented in this work. The integration of the investment dynamic into MILP formulation was depicted. Furthermore, typical days and time blocks were introduced to reduce computational times induced by the multi-stage approach. Next, two case studies were run to demonstrate novelties that could be extracted from this approach compared to the static investment problem. These new aspects could be summarized as follows:

- Investment could be modified along the horizon by taking

full advantage of cost evolution.

- The multi-stage approach not only optimizes the size of technologies, but also determines the investment pathway along the horizon.
- System aging could be controlled as the SoH dynamic is included into optimization.
- The multi-stage approach is able to take time series and parameter evolutions over the 20 years into account thanks to the time block structure.

Finally, the typical day approximation was discussed and it seems that it could be a promising approach which needs to be further explored to reduce computational times when they become a critical issue. In future works, the multi-stage approach will be applied to multi-energy systems with seasonal storage which means that computational times must be further reduced and additional work need to be conducted in that direction. This latter aspect is particularly crucial in order to include uncertainties into the framework.

6. ACKNOWLEDGMENTS

This work has been supported by the ADEME (french national agency on environment, energy and sustainable development) in the framework of the HYMAZONIE project.

7. REFERENCES

[1] D. Connolly, H. Lund, B. V. Mathiesen, and M. Leahy, "A review of computer tools for analysing the integration of renewable energy into various energy systems," *Applied Energy*, vol. 87, pp. 1059–1082, Apr. 2010.

[2] P. Gabrielli, M. Gazzani, E. Martelli, and M. Mazzotti, "Optimal design of multi-energy systems with seasonal storage," *Applied Energy*, vol. 219, pp. 408–424, June 2018.

[3] G. Mavromatidis, *Model-based design of distributed urban energy systems under uncertainty*. Doctoral Thesis, ETH Zurich, 2017. Accepted: 2017-09-11T11:11:22Z.

[4] N. E. Koltsaklis and A. S. Dagoumas, "State-of-the-art generation expansion planning: A review," *Applied Energy*, vol. 230, pp. 563–589, Nov. 2018.

[5] B. Guinot, B. Champel, F. Montignac, E. Lemaire, D. Vannucci, S. Sailler, and Y. Bultel, "Techno-economic study of a PV-hydrogen-battery hybrid system for off-grid power supply: Impact of performances' ageing on optimal system sizing and competitiveness," *International Journal of Hydrogen Energy*, vol. 40, pp. 623–632, Jan. 2015.

[6] R. Rigo-Mariani, B. Sareni, and X. Roboam, "Integrated Optimal Design of a Smart Microgrid With Storage," *IEEE Transactions on Smart Grid*, vol. 8, pp. 1762–1770, July 2017.

[7] P. Carpentier, J.-P. Chancelier, M. D. Lara, and T. Rigaut, "Algorithms for two-time scales stochastic optimization with applications to long term management of energy storage," *hal-02013969*, 2019.

[8] W. Powell, "Energy and Uncertainty: Models and Algorithms for Complex Energy Systems," *AI Magazine*, vol. 35, p. 8, Sept. 2014.

[9] S. Quoilin, K. Kavvadias, A. Mercier, I. Pappone, and A. Zucker, "Quantifying self-consumption linked to solar home battery systems: Statistical analysis and economic assessment," *Applied Energy*, vol. 182, pp. 58–67, Nov. 2016.

[10] P. Haessig, H. Ben Ahmed, and B. Multon, "Energy storage control with aging limitation," in *2015 IEEE Eindhoven PowerTech*, (Eindhoven, Netherlands), pp. 1–6, IEEE, June 2015.

[11] S. Pfenninger, "Dealing with multiple decades of hourly wind and PV time series in energy models: A comparison of methods to reduce time resolution and the planning implications of inter-annual variability," *Applied Energy*, vol. 197, pp. 1–13, July 2017.

[12] H. Teichgraeber and A. R. Brandt, "Clustering methods to find representative periods for the optimization of energy systems: An initial framework and comparison," *Applied Energy*, vol. 239, pp. 1283–1293, Apr. 2019.

[13] G. Limpens, S. Moret, H. Jeanmart, and F. Maréchal, "EnergyScope TD: A novel open-source model for regional energy systems," *Applied Energy*, vol. 255, p. 113729, Dec. 2019.

[14] "Energy Information and Data | OpenEI.org."

[15] W. Holmgren, C. Hansen, and M. Mikofski, "pvlib python: a python package for modeling solar energy systems," *Journal of Open Source Software*, vol. 3, p. 884, Sept. 2018.

[16] "Electricité - Tarif Bleu EDF : Option Base ou Heures Creuses."

[17] N. Lebedeva, D. Tarvydas, and I. Tsiropoulos, "Li-ion batteries for mobility and stationary storage applications: scenarios for costs and market growth.," tech. rep., European commission, Joint Research Center, 2018. OCLC: 1111111915.

[18] IRENA, "Renewable power generation costs in 2018," tech. rep., International Renewable Energy Agency, Abu Dhabi, 2019.